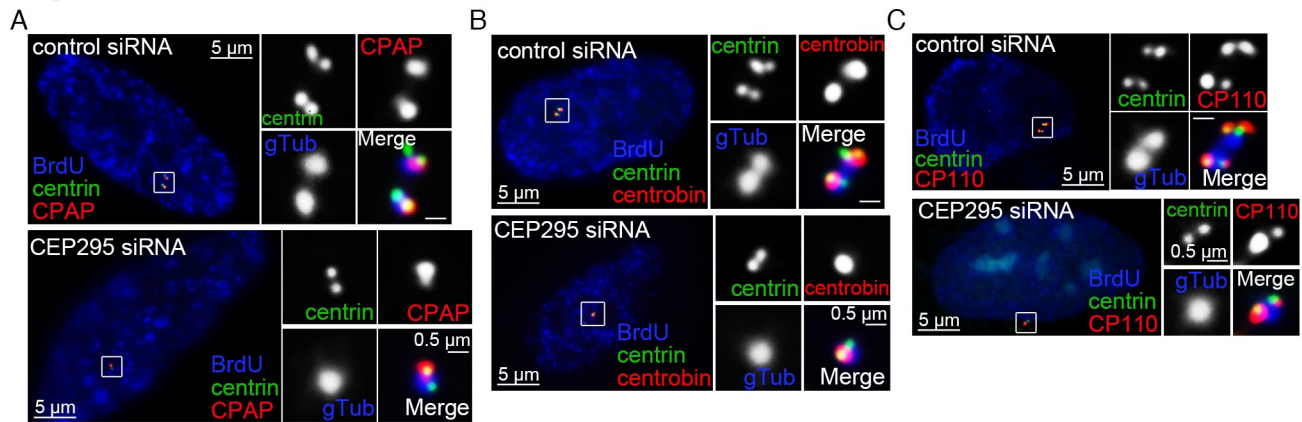


Supplemental Information

Inventory of Supplemental Information

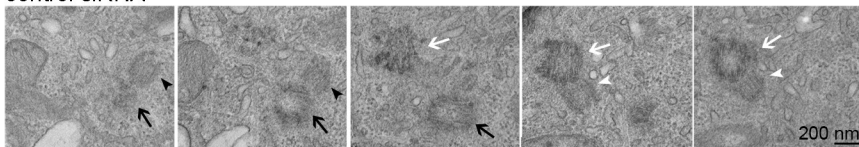
1. Figure S1, related to Figure 2. Loss of CEP295 does not block centriole assembly
2. Figure S2, related to Figure 3. *CEP295*^{-/-}; *p53*^{-/-} cells actively proliferate in the absence of centrosomes
3. Figure S3, related to Figure 4. Cartwheel is required for the maintenance of newborn centrioles formed in the presence of CEP295
4. Movie S1, related to Figure 3. *De novo* centrioles in S phase-arrested *CEP295*^{-/-}; *p53*^{-/-} cells are stable.
5. Supplemental Experimental Procedures
6. Supplemental References

Figure S1

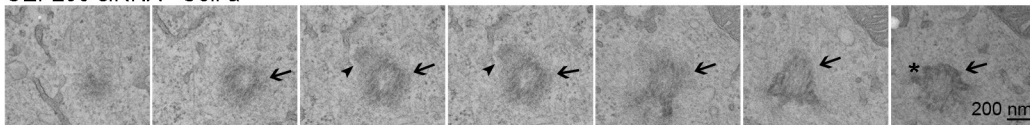


D

control siRNA



CEP295 siRNA - Cell a



CEP295 siRNA - Cell b

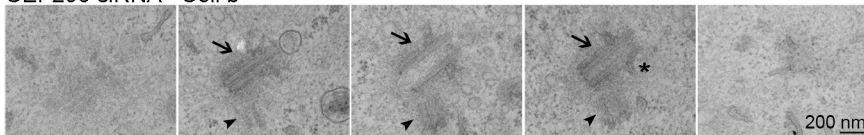
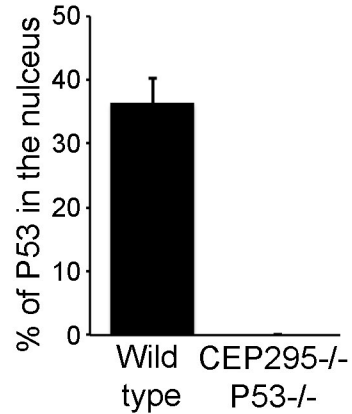
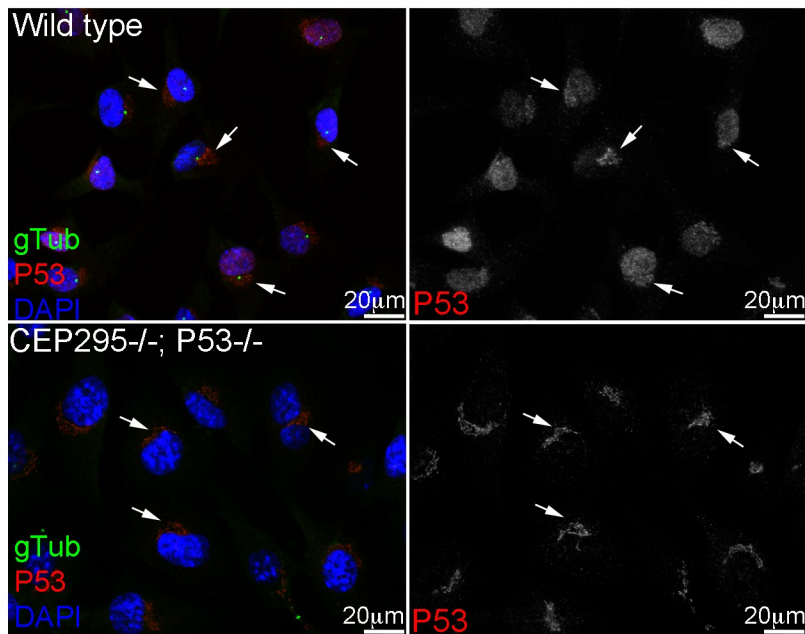


Figure S2

A



B

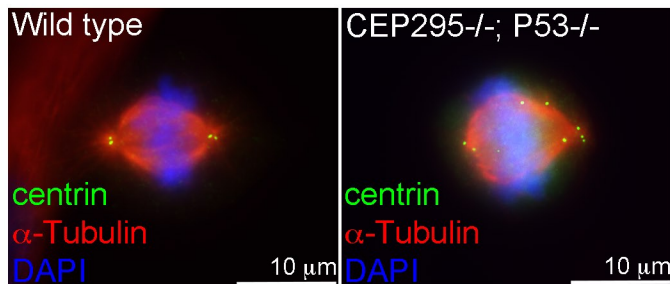
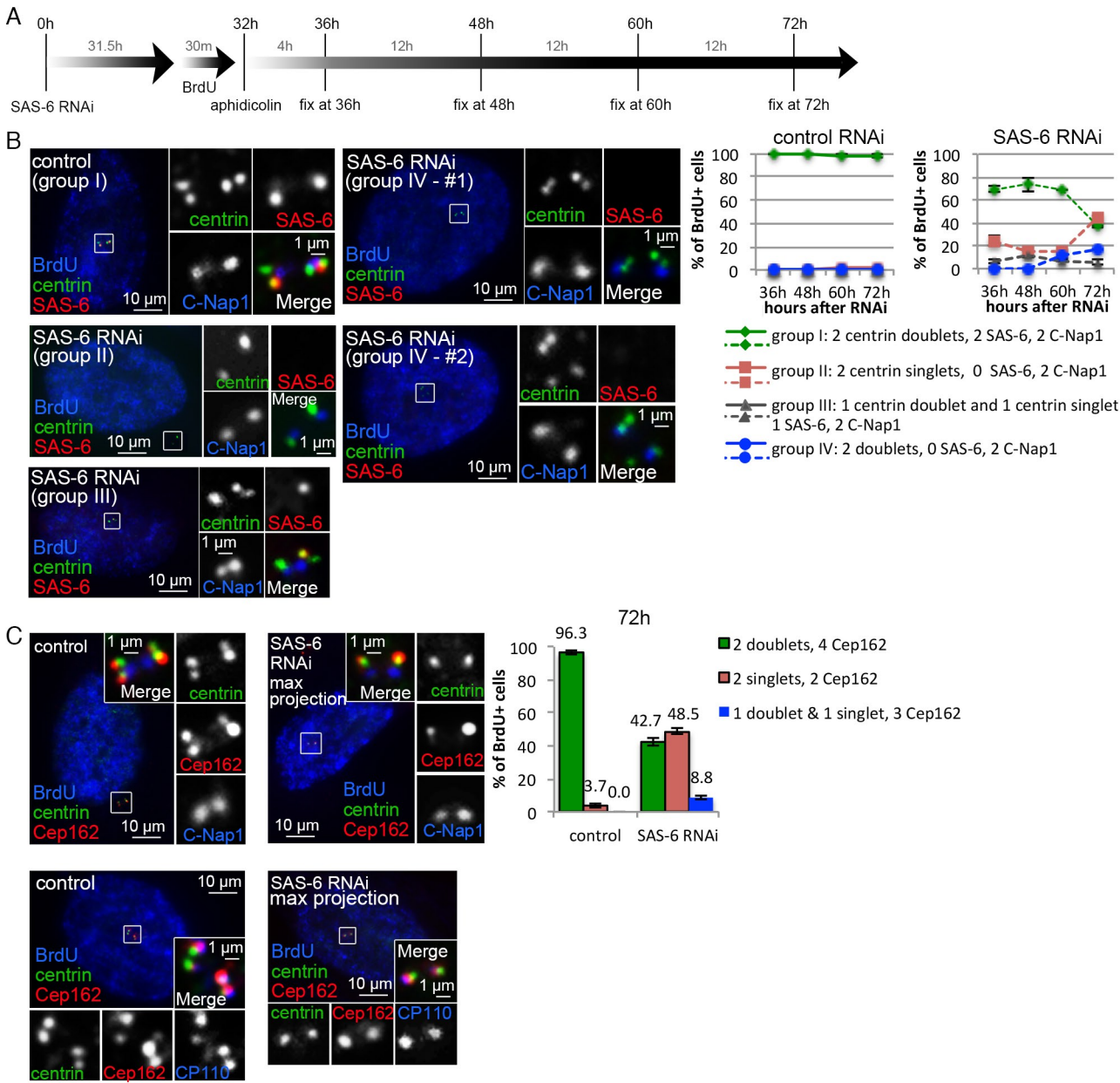


Figure S3



SUPPLEMENTAL FIGURES

Figure S1 (related to Figure 2). Loss of CEP295 does not block initial centriole assembly

(A-C) Centriole duplication was analyzed in control or CEP295-RNAi cells in S phase 72hr after transfection, with antibodies against indicated centriole markers, including CPAP (A), Centrobin (B), and CP110 (C). BrdU marks S-phase cells.

(D) Serial-section electron microscopy analyses of control or CEP295-RNAi cells in S/G2 phase. Serial section images from one control cell (upper) and two CEP295-RNAi cells (a & b; middle and bottom) were shown. Arrows and arrowheads indicate mother and newborn daughter centrioles respectively. Note that in 5 out of 5 control cells in which centriole duplication has occurred, the two duplicated centrioles pairs were closely associated to each other and thus could be easily recovered within a few thin sections. In contrast, in 3 out of 5 CEP295-RNAi cells, only one pair of duplicated centrioles could be recovered from all sections that covered nearly the entire cell, consistent with our IF studies shown in Figure 2. Moreover, without exceptions, the mother centriole identified in CEP295-RNAi cells carried appendages (stars), indicating that it is the older mother centriole that was converted to centrosomes prior to CEP295 depletion.

Figure S2 (related to Figure 3). *CEP295*^{-/-}; *p53*^{-/-} cells actively proliferate in the absence of centrosomes

(A) Centrosomes and nuclear (active) p53 were observed in ~100% and ~35%, respectively, of wild-type cells, but completely absent in *CEP295*^{-/-}; *p53*^{-/-} cells. Wild-type or *CEP295*^{-/-}; *p53*^{-/-} RPE1 cells were stained with antibodies against p53 (red) and γ -tubulin (green). Note that the p53 antibody has non-specific cross-reactivity with the Golgi complex (arrows).

(B) Wild-type or *CEP295*^{-/-}; *p53*^{-/-} cells in metaphase were stained with indicated antibodies to visualize centrioles (centrin) and spindles (α -tubulin). Note that *CEP295*^{-/-}; *p53*^{-/-} cells, which carried de novo centrioles, can divide with bipolar spindles, although the duration of mitosis is prolonged (not shown).

Figure S3 (related to Figure 4). Cartwheel is required for the maintenance of newborn centrioles formed in the presence of CEP295

(A) Schematic outlining the timing of cell manipulation and fixation/collection.

(B) Cells treated with control or SAS-6 RNAi were collected from each indicated time point, examined with antibodies against BrdU, centrin, SAS-6, and C-Nap1 as indicated, and classified into 4 groups based on the phenotypes (group I-IV). Representative images (for the 72h time point only) and quantifications (all time points) for each phenotypic group are shown as indicated. Quantifications were obtained from 3 independent experiments ($n > 100$, $N = 3$). Error bars represent standard deviation.

(C) Maximum projection of a Z-stack ApoTome confocal images sectioning through the whole cell. Control or SAS-6 RNAi cells collected at the 72h time point were examined with antibodies against distal end markers centrin and CEP162 (upper panel), or centrin, CEP162, and CP110 (lower panel). Quantifications of centrin and CEP162 staining are shown on the right ($n > 100$, $N = 3$). Error bars represent standard deviation.

Movie S1 (related to Figure 3). *De novo* centrioles in S phase-arrested $CEP295^{-/-}$; $p53^{-/-}$ cells are stable

$CEP295^{-/-}$; $p53^{-/-}$ RPE1 cells transfected with the centrin::GFP expression construct and arrested in S phase were imaged by time-lapse fluorescence microscopy configured with a 40× objective, using 10 min as the interval time for 10 hours. Images shown in the movie were generated from maximum intensity projections of a z-stack. Movie plays at 2 frames/sec.

SUPPLEMENTAL EXPERIMENTAL PROCEDURES

Cell culture and plasmids

U2OS cells were cultured in DMEM medium with 10% FBS and 1% penicillin-streptomycin. Human telomerase-immortalized retinal pigment epithelial cells (hTERT-RPE1, RPE1) were cultured in DME/F-12 (1:1) medium supplemented with 10% FBS and 1% penicillin-streptomycin. Stable clones of RPE1 cells expressing PLK4 from the tetracycline-inducible promoter were obtained through in vivo gene delivery using the lentiviral vector pLVX-Tight-Puro vector (Clontech). Full-length cDNA of CEP295 was obtained from Kazusa DNA Research Institute and cloned into a pEGFP mammalian expression vector without the GFP. A two-base pair deletion in the open reading frame of the source clone was corrected by site directed mutagenesis (Stratagene).

Drug Treatments

To block cartwheel removal, cells were treated with 200nm BI-2536, or 50 μ m monastrol (Eg5 inhibitor) as the control, for 5 hours. Mitotic arrest cells were released into G1 with 20 μ m roscovitine (Cdk inhibitor) for 16 hours. To arrest cells in S-phase, cells were treated with 2 μ g/mL aphidicolin for the indicated time.

RNAi

Synthetic siRNA oligonucleotides were obtained from Life Technologies. Transient transfection of siRNA oligos into U2OS or RPE1 cells was performed using RNAiMAX (Life Technologies). The 21-nucleotide siRNA sequence targeting CEP295 corresponded to 5'-GUGAUACACUAACAAUUGA -3'. The siRNA sequence targeting SAS-6 corresponded to 5'-GAGCUGUUAAAGACUGGAUACUUUA-3'. The control siRNA was from Silencer[®] Select Negative Control No. 1 (Life Technologies).

CRISPR-mediated gene targeting

RNA-guided targeting of CEP295 in human cells was achieved through coexpression of

the Cas9 protein with one or more gRNAs using reagents prepared by the Church group (Mali et al., 2013), which are available from the Addgene (<http://www.addgene.org/crispr/church/>). Two 23bp genomic targeting sequences for CEP295 gRNAs, 5'-GCTGAGATTGAGTCCTAATGAGG-3' and 5'-GCGAAACTAAGATTGCTACAGG-3', were cloned into the gRNA Cloning Vector (Addgene plasmid #41824) via the Gibson assembly method (New England Biolabs) as described previously (Mali et al., 2013). Both gRNA targeting sequences of CEP295 work well and generate the same phenotypes. RPE1 cells incubated with 5µg Cas9 plasmid (Addgene plasmid #41815) and 5µg gRNA were nucleofected according to manufacturer's instruction (Lonza). Cells were examined for the loss of CEP295 at 5, 6, or 7 days after nucleofection. We consistently see loss of the CEP295 signal, and the associated phenotypes in ~15% of transfected cells. CEP295^{-/-} cells can divide but eventually die through p53 dependent cell death (Bazzi and Anderson, 2014) (not shown). To obtain a stable cell line lacking CEP295, the p53 gene was targeted by the same CRISPR method prior to inactivation of CEP295, generating p53^{-/-}; CEP295^{-/-} cell lines. CEP295^{-/-}; p53^{-/-} cells actively proliferate or divide (Figure S2), but take longer periods of time to go through mitosis (not shown). The genomic targeting sequences for p53 is 5'-GGGCAGCTACGGTTTCCGTCTGG-3'

Antibodies

A rabbit polyclonal antibody against human C-Nap1 was produced as previously described (Tsou and Stearns, 2006). A rat polyclonal antibody against human CEP162 was produced as previously described (Wang et al., 2013). Other antibodies used in this study include anti-CEP295 (ab122490; 1:1000 for immunofluorescence and 1:500 for immunoblotting; abcam); anti-α-tubulin (clone DM1A, 1:2000 for immunoblotting and 1:1000 for immunofluorescence; Sigma-Aldrich); anti-P53 (sc6243; 1:500; SantaCruz); anti acetylated-tubulin (clone 6-11B-1; T7451; 1:2000; Sigma-Aldrich); rat anti-BrdU (1:500; Novus Biologicals); anti-HA (MMS-101P; 1:1000; Covance); anti-CP110 (12780-1-AP; 1:200; Proteintech); anti-γ-tubulin (Tu30; sc-51715; 1:500; Santa Cruz); anti-hSAS-6

(sc-81431; 1:250; Santa Cruz); anti-centrin2 (clone 20H5; 04-1624; 1:1000; Millipore); anti-CPAP (11517-1-AP; 1:1000; Proteintech); anti-ODF2 (clone 1A1; H00004957-M01; 1:100; Novus Biologicals); anti-centrin3 (clone 3E6; H00001070-M01; 1:200; Abnova); mouse anti-C-Nap1 (clone 42; 611374; 1:200; BD Biosciences); anti-centrobin is a kind gift from K. Rhee (Seoul National University, Korea).

Immunofluorescence

Cells were fixed with methanol at -20°C for 10 min or 4% paraformaldehyde at room temperature for 15 min. Slides were blocked with 3% bovine serum albumin (w/v) with 0.1% Triton X-100 in PBS before incubating with the indicated primary antibodies. Secondary antibodies were from molecular probes and were diluted 1:500. DNA was visualized using 4',6-diamidino-2-phenylindole (DAPI; Molecular Probes). Fluorescent images were acquired on an upright microscope (Axio imager; Carl Zeiss) equipped with 100 \times oil objectives, NA of 1.4, and a camera (ORCA ER; Hamamatsu Photonics).

Transmission electron microscopy

Cells grown on coverslips made of Aclar film (Electron Microscopy Sciences) were fixed in 4% paraformaldehyde and 2.5% glutaraldehyde with 0.1% tannic acid in 0.1 M sodium cacodylate buffer at room temperature for 30min, postfixed in 1% OsO_4 in sodium cacodylate buffer for 30min on ice, dehydrated in graded series of ethanol, infiltrated with EPON812 resin (Electron Microcopy Sciences), and then embedded in the resin. Serial sections (~ 90 -nm thickness) were cut on a microtome (Ultracut UC6; Leica) and stained with 1% uranyl acetate as well as 1% lead citrate. Samples were examined on JOEL transmission electron microscope.

Immunoblotting

Cell were lysed in NP-40 lysis buffer (50 mM Tris-HCl at PH 8.0, 150 mM NaCl. 1% NP40) with protease inhibitor for 30 min at 4°C . After centrifugation, cell lysates were resolved by SDS-PAGE and analyzed by immunoblotting using different antibodies as indicated.

Time-lapse microscopy

For correlative time-lapse experiments, cells were grown on gridded coverslips and imaged on a microscope (Axiovert; Carl Zeiss) configured with a 10× phase objective, motorized temperature-controlled stage, environmental chamber, and CO₂ enrichment system (Carl Zeiss). Image acquisition and processing were performed using Axiovision software (Carl Zeiss). 60 fields of cells were filmed with 2 × 2 binning during each experiment.

SUPPLEMENTAL REFERENCES

Bazzi, H., and Anderson, K.V. (2014). Acentriolar mitosis activates a p53-dependent apoptosis pathway in the mouse embryo. *Proceedings of the National Academy of Sciences of the United States of America* *111*, E1491-1500.

Mali, P., Yang, L., Esvelt, K.M., Aach, J., Guell, M., DiCarlo, J.E., Norville, J.E., and Church, G.M. (2013). RNA-guided human genome engineering via Cas9. *Science* *339*, 823-826.

Tsou, M.F., and Stearns, T. (2006). Mechanism limiting centrosome duplication to once per cell cycle. *Nature* *442*, 947-951.

Wang, W.J., Tay, H.G., Soni, R., Perumal, G.S., Goll, M.G., Macaluso, F.P., Asara, J.M., Amack, J.D., and Bryan Tsou, M.F. (2013). CEP162 is an axoneme-recognition protein promoting ciliary transition zone assembly at the cilia base. *Nature cell biology* *15*, 591-601.